A magnetic biocatalyst based on mussel-inspired polydopamine and its acylation of dihydromyricetin

DENG, Xiao, CAO, Shilin, LI, Ning, WU, Hong, SMITH, Thomas <http://orcid.org/0000-0002-4246-5020>, ZONG, Minhua and LOU, Wenyong

Published version

DENG, Xiao, CAO, Shilin, LI, Ning, WU, Hong, SMITH, Thomas, ZONG, Minhua and LOU, Wenyong (2016). A magnetic biocatalyst based on mussel-inspired polydopamine and its acylation of dihydromyricetin. Chinese Journal of Catalysis, 37 (4), 584-595.

Preparation of a magnetic nanobiocatalyst based on mussel-inspired polydopamine and its efficient application to acylation of dihydromyricetin

Xiao Deng [a, c‡], Shi-Lin Cao [b,c‡], Ning Li [c], Hong Wu[c], Thomas J Smith [d,], Min-Hua Zong [a,b], Wen-Yong Lou [a,c *]**

[a] State Key Laboratory of Pulp and Paper Engineering, South China University of Technology, Guangzhou 510640, China

[b] School of Chemistry and Chemical Engineering, South China University of Technology, Guangzhou 510640, China

[c] Lab of Applied Biocatalysis, School of Light Industry and Food Sciences, South China University of Technology, Guangzhou 510640, China

[d] Biomolecular Sciences Research Centre, Sheffield Hallam University, Owen Building, Howard Street, Sheffield, S1 1WB, UK

*Corresponding author. Tel.: +86-20-22236669. E-mail address: wylou@scut.edu.cn (W.-Y. Lou)

**Corresponding author. E-mail address: t.j.smith@shu.ac.uk (T. J. Smith)

‡Xiao Deng and Shi-Lin Cao are co-first authors to this work.

ABSTRACT

A mussel-inspired polydopamine-coated magnetic iron oxide nanoparticles (PD-MNPs) hybrid composite was successfully prepared and structurally characterized in detail. A widely used *Aspergillus niger* lipase (ANL) was effectively immobilized onto PD-MNPs (ANL@PD-MNPs), with a protein loading of 138 mg/g-support and an activity recovery of 83.6% at optimal conditions. During the immobilization process, the pH and the immobilization time were investigated respectively. Meanwhile, the pH, thermal and storage stabilities of ANL@PD-MNPs significantly surpassed those of free ANL. Also, ANL@PD-MNPs manifested better solvent tolerance than free ANL and secondary structure of free ANL and ANL@PD-MNPs was analyzed by infrared spectroscopy. A kinetic study demonstrated that the as-prepared ANL@PD-MNPs had an enhanced enzyme-substrate affinity and a relatively high catalytic efficiency. Furthermore, the prepared ANL@PD-MNPs was successfully applied as an efficient nanobiocatalyst for regioselective acylation of dihydromyricetin (DMY) in DMSO with a conversion of 79.3%, which was higher than that reported previously. The as-prepared ANL@PD-MNPs remained over 55% of its initial activity after 10 cycles of consecutive reuse. Besides, the ANL@PD-MNPs was readily separated from the reaction system by magnetic forces. Clearly, PD-MNPs is a excellent support for ANL and the resulting ANL@PD-MNPs displayed great potential for efficient synthesis of dihydromyricetin-3-acetate through enzymatic regioselective acylation.

Keywords: magnetic iron oxide; nanoparticles; polydopamine; *Aspergillus niger* lipase; acylation; dihydromyricetin

1.Introduction

As an important biological catalyst, lipase (glycerol ester hydrolases E.C.3.1.1.3) is widely used in the production of biofuels, organic synthetic compounds, detergents, perfumes, cosmetics, leather, enantiopure pharmaceuticals, medical diagnostics, foods and feeds[1, 2]. *Aspergillus niger* lipase is a well known biocatalyst because of its wide application in the chemoselective, enantioselective and regioselective hydrolysis and synthesis of a broad range of non-natural esters[3]. However, the disadvantages of the free lipase, such as poor mechanical stability, unrecyclability and difficulties in separating from products, hinder its further application in industry. To overcome these problems, immobilization techniques of enzyme have been widely employed[4]. With the further development of catalytic system, the ideal immobilization methodology should meet the following reqirements: (i) The enzyme carrier should manifest a high specific surface area, good biocompatibility, be easily recyclable and capable of binding large amounts of enzyme with recovery of enzymatic activity. (ii) The immobilization process should be simple, rapid and facile. (iii) The immobilized enzyme should exhibit good stability in the reaction system[5].

In recent years, magnetic iron oxide nanoparticles (MNPs) have attracted great interest owing to its properties, such as biocompatibility, superparamagnetism, high

surface-to-volume ratios and low toxicity[6]. It has been used as enzyme supports due to its high specific surface area and easy separation from the reaction mixture by an external magnetic field[7]. In most cases, the MNPs require further modification or functionalization to introduce catalyst on the surface.

Polydopamine, a polymer inspired by the composition of adhesive protein in mussels, is one of the most commonly used biomimetic materials[8]. The primary advantage of polydopamine is that, it can be easily deposited on virtually all types of inorganic and organic materials by the self-polymerization of its monomer dopamine[9-11]. Furthermore, polydopamine could graft some macmoleculars (such as enzyme) containing thiol or amine via Michael addition or Schiff base reaction between catechols (a moiety of polydopamine or dopamine) and amines or thiols[12]. Therefore, it is of great interest to make use of polydopamine to surface modify MNPs, and the polydopamine-coated MNPs (PD-MNPs) can be a excellent carrier for enzyme immobilization[13] due to these advantages: polydopamine exhibit good biocompatibility; the enzyme immobilization process is simple and wild [14, 15]; the as-prepared immobilized enzyme could be easily and rapidly recycled from the reaction system through the magnetic force.

Dihydromyricetin (DMY), a natural aglycone flavonoid, has been found to possess numerous bioactivities with potential beneficial effects to the human body, such as anti-inflammatory, analgesic, antitussive, expectorant, antibacterial, anti-thrombotic and anti-tumor activities[16]. However, DMY is poorly soluble in

both aqueous and nonaqueous systems, which limits its processability and application potential. Lately, Hou et al[17] in our research group firstly reported the lipase catalytic acylation of DMY, and the solubility of product in organic solvents and lipid systems was significantly improved. Nevertheless, to meet the requirements in industrial production, the reusability of the lipase needed to be significantly improved.

In this study, the MNPs were successfully prepared and surface modified with polydopamine coating. Then, the polydopamine-coated MNPs (PD-MNPs) were structurally characterized in detail. Furthermore, the lipase from *Aspergillus niger* (ANL) was successfully immobilized onto the PD-MNPs with relatively high recovery activity and protein loading for the first time. Also, the enzymatic properties of the resulting immobilized lipase (ANL@PD-MNPs) were investigated systematically. Finally, for the first time, the as-prepared ANL@PD-MNPs was used as a magnetically recyclable biocatalyst for the kinetic regioselective acylation of dihydromyricetin (DMY).

2. Experimental Section

2.1. Materials

Dopamine hydrochloride was purchased from Aladdin. Ferric chloride hexahydrate ($FeCl_3 \cdot 6H_2O$) and ferrous chloride tetrahydrate ($FeCl_2 \cdot 4H_2O$) were from the Guangzhou Chemical Reagent Co. Ltd. *Aspergillus niger* lipase was purchased from Shenzhen Leveking Bio-Engineering Co. Ltd(Shenzhen, China). DMY was from Aladdin (Shanghai, China). Vinyl acetate (VA), used as acyl donor, was purchased from

Sigma-Aldrich and TCI Co. Ltd. (Shanghai, China). All other reagents were analytical reagents and obtained from commercial sources.

2.2. Preparation of MNPs

The procedure for the preparation of MNPs is based on the conventional co-precipitation method with some modifications. In a typical experiment, 0.9 g $FeCl_2 \cdot 4H_2O$ and 2.43 g $FeCl_3 \cdot 6H_2O$ were dissolved in 300 mL deionized water under nitrogen at room temperature; then the pH of the solution was kept at 9.5 using 25% ammonia solution with vigorous stirring. After 1 hour, the magnetite precipitates were collected by external magnetic force and washed three times with deionized water. The precipitate was dispersed in Tris-HCl buffer (10mM, pH 8.5) to 2.7 mg MNPs per milliliter of solution.

2.3. Preparation of PD-MNPs

Firstly, the MNPs suspension prepared as described above was ultrasonicated for 20 minutes before dopamine hydrochloride (37.5 mg, 2.5 mg/mL) was added to the MNPs suspension. Then the pH of the solution was adjusted to 8.5 by addition of 100 mM NaOH. After vigorous stirring for1 hour, the PD-MNPs was separated by external magnetic field and washed three times with deionized water and then dispersed in deionized water to 4.2 mg PD-MNPs per milliliter solution.

2.4. Immobilization of *Aspergillus niger* lipase on the PD-MNPs

Before immobilization, the PD-MNPs solution was ultrasonicated for 10 minutes. In order to immobilize *Aspergillus niger* lipase (ANL), the suspension of PD-MNPs

was added to a buffered lipase solution. An aqueous solution of ANL (1.5 mg/mL) was prepared by dissolving the ANL powder in sodium phosphate (50mM, pH 8.0) solution. The freshly prepared PD-MNPs solution (2 mL, 4.2 mg/mL) was added to the ANL solution (1 mL, 1.5 mg/mL) at 0°C in an ice bath. After stirring at 100 rpm for 12 h (at 0°C), the ANL-loaded precipitates were washed and collected with deionized water. Then, the concentration of the residual ANL in the solution and the concentration of ANL in the washings were determined by the Bradford method [18]. The amount of ANL in the prepared ANL@PD-MNPs was calculated using the following equation:

$$\text{amount of ANL on ANL@PD-MNPs} = m\text{-}C_1V_1\text{-}C_2V_2$$

where m (mg) represents the mass of ANL initially added to the solution, C_1 (mg/ml) represents the residual ANL concentration of the solution, V_1(ml) represents the volume of the solution, C_2 (mg/ml) represents the ANL concentration of the washings, V_2 (ml) represents the volume of the washings. Finally the ANL@PD-MNPs was stored at 4°C prior to use.

2.5. Activity assay of free ANL or ANL@PD-MNPs

The enzymatic activities of free and immobilized lipase were measured by the *para*-nitrophenyl palmitate (*p*NPP) assay[19]. The basis of this assay protocol is the colorimetric estimation of *para*-nitrophenol (*p*NP) released as a result of enzymatic hydrolysis of *p*NPP at 405 nm. In brief, a given amount of free lipase or immobilized lipase was dispersed in 0.6 mL of sodium phosphate (50 mM, pH 7.0) solution and

subsequently mixed with 0.1 mL of 140mM *para*-nitrophenyl palmitate (in isopropanol) as the substrate. After 5 minutes of incubation at 35°C with shaking at 100 rpm, the enzymatic reaction was terminated by the addition of 5.3 mL of ethanol and the free *para*-nitrophenol was detected spectrophotometrically at 405 nm. One unit (U) of lipase activity was defined as the amount of lipase which liberated 1 μmol of *para*-nitrophenol per minute under the assay conditions. The activity recovery of the immobilized enzyme was calculated as the ratio of immobilized lipase activity to that of the amount of lipase added initially.

2.6. Characteristics of free ANL and ANL@PD-MNPs

In order to study the optimal pH and temperature of both free and immobilized lipases, the activities were measured over the pH range from 5 to 10 and the temperature range from 20°C to 80°C.

The Michaelis-Menten constant (K_m) and the maximum reaction rate (V_{max}) of both free and immobilized lipases, as well as the reusability of the immobilized lipase, were determined as described previously[20]. In order to assay the kinetic parameters of free and immobilized lipases, the enzymatic hydrolysis of *p*NPP was used as the model reaction. The initial reaction rates were determined under optimum reaction conditions (0.063U of enzyme per mL, 35°C, pH 7.0 for the free enzyme or 40°C, pH 8.0 for the immobilized enzyme). The substrate concentrations was varied from 20 to 180 mM. The Michaelis-Menten equation was used to fit the data (initial reaction rate *vs.* substrate concentration), and the kinetic parameters (K_m and V_{max}) of *p*NPP

hydrolysis with free or immobilized lipase were obtained from the fit.

To determine the pH stability and thermostability of the enzyme, lipase-immobilized-PD-MNPs containing 20 μg lipase or 20 μg free lipase were incubated in sodium phosphate buffer (50 mM) adjusted to various pH values (pH 6-10 at 40°C) and various temperatures (40-80°C, pH 7). The incubation times to test the stability of the enzyme were 12 h and 8 h for the pH stability and thermostability, respectively. The residual activity of both free and immobilized lipases was determined as above.

To investigate the solvent tolerance of the free and immobilized enzymes, lipase immobilized on MNPs containing 50 U lipase or 50 U free lipase were incubated in 3 mL of solvent (acetonitrile, DMSO, ethanol or [HMIm]BF_4) at 30°C for 6 h and the residual activity of the enzyme was assayed via the method described above.

2.7. Secondary structure analysis of free ANL and ANL@PD-MNPs by infrared spectroscopy

The IR spectra of free ANL and ANL@PD-MNPs were obtained through the same method described before. FTIR spectra were detected from 4000 to 400 cm^{-1} with powder samples dispersed in the pressed KBr discs using a Tensor 37 spectrometer (Bruker, Germany) equipped with a deuterated triglycine sulfate (DTGS) detector. This equipment system was managed by Bruker OPUS software. Besides, subtraction of residual vapour absorption was also performed as necessary. And the the background spectra were recorded in absence of the enzyme. The enzyme spectras

were corrected by subtraction of the background spectra. Curve fitting of the amide I region (1600 to 1700 cm-1), were smoothed with a 13-point Savitzky-Golay and identified using the secondary derivative. Then, a multipeak fitting program with Gaussian function in PeakFit 4.2 software (Jandel Scientific) was used to quantitatively evaluate the multicomponent peak areas in protein amide I bands. The relative contents of α-helix structure (1650 cm^{-1}-1658 cm^{-1}), β-sheet structure (1610cm^{-1}-1640 cm^{-1}), random coil structure (1640 cm^{-1}-1650 cm^{-1}), and β-turn structure (1660cm^{-1}-1700 cm^{-1}) based on the multicomponent peak area were calculated according to the previous literature by the software[21].

2.8. Application of ANL@PD-MNPs to the regioselective acylation of DMY

During the regioselective acylation process of DMY, 60 U of free ANL or ANL@PD-MNPs was added to 2 mL of DMSO, followed by the addition of DMY and vinyl acetate to the final concentrations of 0.04 mM and 0.4 mM, respectively. The mixture was incubated 35°C in an orbital shaking water bath (200 rpm) for up to 48 h. Aliquots were withdrawn at specified time intervals. The reaction mixtures were analyzed by RP-HPLC on a 4.6 mm × 250 mm (5 μm coating thickness) Zorbax SB-C18 column (Agilent Technology Industries Co., Ltd.) using a Waters HPLC system consisting of two Waters 1525 pumps and a Waters 2489 UV detector set at 294 nm. Elution was performed with a gradient system comprising 0.1% acetic acid and 100% methanol as solvents A and B, respectively. Elution began with 28% solvent B, which was increased to 30% between 0 and 6 min, and then to 80%

between 6 and 12 min, and finally returned 28% between 12 and 13 min. The peak of DMY (which eluded at 6.68 min)was detected by HPLC. The conversion (C) of DMY was calculated as per formula (1):

$$C\ (\%) = \frac{C_0 - C_S}{C_0} \times 100 \qquad (1)$$

where C_0 and C_S were the initial and terminal concentration of DMY, respectively.

To study the effect of the molar ratio of vinyl acetate to DMY on the reaction, acylation reactions were conducted in 2 ml DMSO with the addition of 60 U free ANL or ANL@PD-MNPs, while the molar ratio of vinyl acetate to DMY was varied from 2.5 to 25.To investigate the effect of temperature on the reaction, acylation reactions were conducted under the same conditions as above except that the molar ratio of vinyl acetate to DMY was fixed at 1 to 10 (0.04 mM DMY and 0.4 mM vinyl acetate) while the reaction temperature was varied between 30 and 50 °C. To study the effect of enzyme concentration on the reaction, acylation experiments were conducted under the same conditions as above except that the temperature was fixed at 45 °C, the molar ratio of DMY to vinyl acetate was fixed at 1 to 10 (0.04 mM DMY and 0.4 mM vinyl acetate), while the amount of enzyme was varied from 10 U to 100 U.

The operational stability of immobilized lipase during the regioselective acylation process of DMY was studied under the same conditions as described in the previous section. After each enzyme run, the ANL@PD-MNPs were magnetically isolated and washed with hexane and ultrapure water to remove any remaining substrate and product species before the next experiment. The residual activity of the immobilized lipase after each cycle was expressed as a percentage of the activity at the beginning of

the experiment.

All data reported in this study were averages of experiments performed at least in triplicate, with no more than 3.0% experimental error.

3. Results and Discussion

3.1. Synthesis and analysis of MNPs and PD-MNPs

TEM images of MNPs and PD-MNPs are shown in Fig. 1. MNPs were spherical shape with the average diameter of 10 nm (Fig. 1A). The fact that the MNPs were aggregated was consistent with their having a large specific surface area and high surface energy. After coating with polydopamine (polymerization time 1 h), it could be clearly observed that the dark MNPs were uniformly encapsulated in light gray polydopamine layer (Fig. 1B). The MNPs showed a tendency to aggregate due to the interaction between polydopamine and MNPs. The average thickness of the polydopamine coating around the edge of the MNP aggregates in the hybrid material was about 4 nm. Fig. 1C showed the TEM image of ANL@PD-MNPs. The mean size of the aggregates of PD-MNPs with immobilized lipase is about 25 nm, which is obviously larger than that of PD-MNPs without the enzyme. Furthermore, the size of MNPs, PD-MNPs and ANL@PD-MNPs was evaluated by dynamic light scattering (DLS). The size distribution was clearly depicted in Figure 1, and the mean sizes of MNPs, PD-MNPs and ANL@PD-MNPs were 9.6, 13.8 and 26.1 nm respectively, which were consistent with those in the TEM images.

XPS was applied to investigate the chemical elements on surface of MNPs and

PD-MNPs. The energy scale was calibrated with the C1s peak of carbon (284.8 eV). Wide-scan XPS spectra for MNPs and PD-MNPs are shown in Figure S1A and Figure S1B of the Supporting information, respectively. The characteristic peaks of Fe2p (Fe $2p_{1/2}$ 724.38 eV, Fe $2p_{3/2}$ 710.58 eV) and O1s (530.08 eV) appeared in the spectrum due to Fe_3O_4, and the weak peak of C1s was attributed to the presence of impurities[22]. After the MNPs were coated with polydopamine, the peak of C1s enhanced significantly (boxed in red in Figure S1B of the Supporting Information), and that of O1s shrank somewhat due to the high content of carbon and low content of oxygen in polydopamine. Meanwhile, the appearance of the characteristic N1s weak peaks at expected positions 399.08 eV (also boxed in red in Figure S1B of the Supporting Information) confirmed the presence of nitrogen contained within the polydopamine. The data in Figure S1B indicate that the PD-MNPs exhibited an N/C ratio of 0.106, which is close to the N/C ratio of 0.125 (dopamine). Figure S1C and Figure S1D show high-resolution scan spectra of the C1s and N1s regions, respectively, of PD-MNPs after XPS peak-differentiating and imitating. The C1s peak contains C–C (284.8 eV), C–N (285.8 eV), C–O (286.3eV) and C=O (287.8eV) peaks and the N1s region is made up of N–H (398.7 eV) and –N= (399.7 eV) peaks, which are in accordance with the previously published XPS results of polydopamine[23]. Taken together, the XPS results demonstrated that MNPs were successfully covered by polydopamine.

The FTIR spectra displayed in Fig. 2 were recorded to confirm the chemical composition of the PD-MNPs. A strong peak appearing at around 580 cm^{-1} and a weak

one at approximately 436 cm^{-1} in the spectra of both the MNPs and PD-MNPs (spectra a and b, respectively in Fig. 2) were related to the vibration of the Fe–O functional group. The relatively high intensity of the band at 580 cm^{-1} indicated the high content of Fe_3O_4[24]. Additionally, a weak band appearing at 1255 cm^{-1} in spectrum b in Fig. 2 was attributed to the phenolic hydroxyl group stretching mode of polydopamine layer. For PD-MNPs, this signal appeared showing the interaction between hydroxyl and aromatic rings. The vibrational signals at 1610 and 1490 cm^{-1} were ascribed to C=C in aromatic rings. The peak at 1428 $cm^{-1}$of PD-MNPs (b) was broader than that of MNPs (a), which results from the overlapping of O=C-O symmetric vibration (1405 cm^{-1}) and the indoline peak of polydopamine (1438 cm^{-1}) [25].

Fig. 3a shows the XRD patterns of the MNPs. Similar to the previous report[26], the XRD pattern showed six diffraction peaks in the 2θ range of 20°–70°, including a high-intensity sharp peak at 2θ = 35.6°, corresponding to the (3 1 1) plane, and five additional weak peaks at 2θ = 30.6°, 43.4°, 54.4°, 56.7° and 62.7°, corresponding to the (2 2 0), (4 0 0), (4 2 2), (4 1 1) and (4 4 0) planes, respectively, showing the presence of the magnetite crystal with a cubic spinal structure[27]. The unit cell of cubic spinal structure consists of eight ferric ions at tetrahedral sites each with four oxide ions nearest neighbors, and eight ferric ions and eight ferrous ions at octahedral sites each with six oxide ions as the nearest neighbors[28]. The XRD spectrum of the PD-MNPs (Fig. 3b) showed that the crystal structure of Fe_3O_4 was maintained after the coating process. No obvious diffraction peak for the polydopamine was observed,

which may be due to the relatively thin layer and amorphous crystallinity of the polydopamine prepared under this polymerization method[29].

The polydopamine, MNPs and PD-MNPs were analyzed via TGA analysis in a nitrogen atmosphere with a heating rate of 10 °C /min. Figure S2 of the Supporting Information illustrates the TGA curves, depicting the variations of the residual masses of the samples with temperature. The first weight loss stage (below 130 ◦C) in the polydopamine sample (Figure S2A(a)) can be ascribed to the evaporation of water molecules in the polymer matrix while the other stage of weight loss, beginning at about 190 ◦C, was due to the decomposition of polydopamine. As the polydopamine (PD) content of the materials increased (Figure S2A(c-e)), the proportion of the mass lost due to thermal decomposition of the PD increased also. As shown in Figure S2B, when the concentration of dopamine hydrochloride is up to 4mg/mL, the weight loss of the PD-MNPs upon heating was 24.4%.

The PD-MNPs could be separated and purified from the solvent by using a magnet (Figure S3A of the Supporting Information). Vibrating specimen magnetometer (VSM) magnetization curves of MNPs and PD-MNPs (Figure S3B) indicated no remanence or coercivity, suggesting that MNPs and PD-MNPs behaved in a superparamagnetic fashion. Saturation magnetization is defined as the maximum magnetic response of materials attained under an external magnetic field, which can be seen as a value to estimate the magnetism of materials[30, 31]. Consistent with their superparamagnetic behavior, the MNPs and PD-MNPs showed high saturation magnetization of 60.1 and

52.7 emu/g, respectively. The lower saturation magnetization of PD-MNPs compared with the MNPs is consistent with their lower proportion of magnetic material due to the presence of the polydopamine coating. Nonetheless, the magnetic properties of PD-MNPs are sufficient to provide an easy and effective way to isolate them from a liquid reaction system.

3.2. Immobilization of free ANL onto PD-MNPs

During the immobilization process, the activity recovery and the protein loading were found to be affected by pH and immobilization time. Therefore, these two factors were varied in order to maximize immobilization capacity and enzyme activity. As the pH was increased from 6 to 9, the amount of lipase that immobilized onto the PD-MNP support increased from 26.3 mg/g of PD-MNP to 138.1 mg/g of PD-MNP. The proportion of the enzyme activity remaining after immobilization dropped off above pH 8 (Fig. 4A). Hence, under the conditions tested pH 8 appears optimal for immobilization of the enzyme because, whilst protein immobilization contuse to become more effective with increasing pH beyond this, the enzyme begins to become inactivated. Immobilization time also influenced the properties of the immobilized biocatalyst. As the immobilization time was increased, the amount of enzyme that loaded onto the PD-MNPs and the proportion of activity remaining after immobilization showed maximum values after 12 h of immobilization, with 138mg/g of enzyme immobilized and 83.6% retention of activity (Fig.4B).The decrease in retention of activity after longer immobilization time may be related to steric

hindrance of substrate access to the enzyme at high enzyme loading onto the solid support [32].

3.3. Characteristics of free ANL and ANL@PD-MNPs

Immobilization resulted in a change in the pH activity profile of the lipase (Fig. 5A), such that the range over which the lipases retained more than 85% of enzyme activity was widened slightly from pH 7 to 8 for the free ANL to pH 7 to 8.5 for the ANL@PD-MNPs, and the optimum pH shifted from pH 7 to 8 upon immobilization. The interactions between the enzyme and the polymeric matrix, such as hydrogen bonding and electrostatic interactions, may explain the observed alkaline shift and broadening in the pH profile of the immobilized lipase[33]. Similar results upon immobilization of lipase and other enzymes have been reported previously [34]. In particular, compared with free ANL, ANL@PD-MNPs exhibited a considerably higher relative activity at pH 10 (64.3% of the maximum activity), while its free counterpart merely had 24.6% of the maximum activity at this pH. Hence, the ANL@PD-MNPs exhibited improved activity across a wider a pH range especially in weakly alkaline media.

Fig.5B shows the effect of temperature on the activity of free ANL and ANL@PD-MNPs. The activity obtained in a temperature range of 20-80°C were expressed as percentage of the maximum activity recorded at 35°C and 40°C for both free ANL and ANL@PD-MNPs, respectively (i.e. as a percentage of the activity at the optimum temperature for each form of the enzyme). Above 50°C, the relative activity

of free ANL dropped sharply and it retained only 26.7% at 80°C. In contrast, ANL@PD-MNPs retained about 54.4% of the relative activity at 80°C. The increase in the optimum temperature of the immobilized enzyme might result from the changing conformational integrity of the lipase structure by covalent bond formation between the enzyme and solid support via amino groups. During the immobilization process, if the flexibility of the enzyme molecules is decreased, the enzyme may require a higher activation energy to reorganize to the appropriate conformation for catalysis[35]. ANL@PD-MNPs showed enhanced heat resistance at high temperature (>70 ºC), possibly because of restricted conformational mobility of the molecules which may protect against thermal denaturation[36]. Therefore, the ANL@PD-MNPs was higher than its free counterpart under high temperatures. Similar observations of improved activity at high temperatures after enzyme immobilization have also been observed[37].

In order to study the pH-stability of the free ANL and ANL@PD-MNPs over a period of time, the enzyme was incubated at 40 °C for 12 h in phosphate buffer (50 mM, pH varied over the range 6–10) (Fig. 6A). The ANL@PD-MNPs retained 49.1% of its initial activity after 12 h incubation at pH 10 (Fig. 6A), while the final activity of the free ANL was only about 22.9 % of the initial value (Fig. 6A), indicating that the ANL@PD-MNPs exhibited enhanced pH stability.

The thermal stability of free ANL and ANL@PD-MNPs were investigated as a function of time at different temperatures between 40°C and 80°C. As seen in Fig.6B,

the ANL@PD-MNPs retained more than 83.5% of its initial activity after incubation for 8 h at 40 °C, while less than 71% of residual activity was detected with the free ANL after the same treatment. As mentioned above, the conformational rigidity of lipase may have been strengthened by immobilization, thus enhancing its thermal stability.

Both free ANL and ANL@PD-MNPs were stored at 4 °C in pH=7 phosphate buffer for 20 days in order to investigate the enzymatic storage stability. Compared to the free ANL, the ANL@PD-MNPs exhibited excellent retention of activity under these conditions, as can clearly be seen by the fact that after 20 days of storage the ANL@PD-MNPs retained 92.8% of its original activity, while the free counterpart retained only 21.5% under the same conditions (Fig.6C).

Compared with the free ANL, the ANL@PD-MNPs exhibited significantly better tolerance to all four solvents tested (Fig.6D). The difference in retention of activity between the free ANL and ANL@PD-MNPs increased with overall degree of inhibition caused by the solvent during the 6 h incubation period at 40°C. Hence, the least inhibitory solvent ethanol permitted retention of 90.48% and 81.30% of the initial activity by the free ANL and ANL@PD-MNPs, respectively. In contrast after exposure to the most inhibitory solvent (the ionic liquid [HMIm]BF_4), the ANL@PD-MNPs retained 63.19% of its initial activity, whereas the free ANL retained only 35.79% of its initial activity. Owing to immobilization, the ANL@PD-MNPs maintained its catalytic conformation and exhibited more structural rigidity, resulting in enhanced solvent tolerance, which is similar in the previous reports[38].

The kinetic behavior of free ANL and ANL@PD-MNPs catalyzing *p*NPP hydrolysis were investigated and both reactions were found to follow Michaelis–Menten kinetics (Figure S4). K_m for free and immobilized lipases were 74.5 and 63.2 mmol/L, respectively, which demonstrated that the immobilized lipase had moderately enhanced enzyme–substrate affinity[39]. The V_{max} for ANL@PD-MNPs and the free ANL were 2.36×10^{-2} m mol L^{-1} min^{-1} and 3.03×10^{-2} m mol L^{-1} min^{-1}., indicating a rather lower maximal rate for the ANL@PD-MNPs compared with the free ANL. This was consistent with the fact that the specific activity of ANL@PD-MNPs was lower than that of the free ANL (1.58 vs. 2.11 U per mg).

The deconvolution of the amide I band from the FTIR spectrum of the free lipase (Figure S5A) has several distinct Lorentzian peaks. The band at 1628.41cm^{-1} can tentatively be assigned to β-sheet structure[40]. Following this assignment and according to deconvolution results, the β-sheets contribution constitutes 26.15% of the secondary structures in free lipase. The band around 1656.24 cm^{-1} is characteristic of an α-helical structure, and the area of this component accounts for 26.14% of the total band area in free lipase. The random coli (about 30%) and β-turns (about %) contribute to the bands at 1646.74 and 1679.74 cm^{-1}, respectively, in the free lipase[41]. In the immobilized lipase (Figure S5B), the Lorentzian bands of the deconvoluted amide I region around 1621.04 and 1634.83cm^{-1} indicate 26.99% of the structure as β-sheets (26.99%) and the band at 1657.80 cm^{-1} suggests an α-helix content of 28.88%. This suggests an increase of β-sheet and α-helix content upon lipase immobilization of 2.74

and 0.84 percentage points, respectively (Table 1). The existence of hydrogen bonds within secondary structure elements such as β-sheet and α-helix generally helps to maintain protein structure[42, 43], which may be one of the reasons why the immobilized lipase exhibited enhanced stability and improved tolerance to organic solvents and ionic liquid[44].

3.4. Application of the ANL@PD-MNPs to the regioselective acylation of DMY

As shown in Fig.7A, when the ANL@PD-MNPs was used as the biocatalyst for acylation of DMY, the time course for the regioselective acylation reaction was similar to that catalyzed by an equal number of units of the free enzyme. The final conversion was 79.28% at 48 h with the immobilized enzyme as biocatalyst and 69.47% with the free enzyme. The greater conversion with the immobilized lipase could be explained by the better organic solvent tolerance of the immobilized enzyme.

As seen in Fig.7B, the molar ratio of substrates strongly affected the conversion rate of enzymatic DMY acylation, With the increase of the molar ratio between vinyl acetate and DMY from 2.5 to 10, the conversion rate increased sharply from 16.1% to 65.3% (free ANL) and 20.3% to 70.6% (ANL@PD-MNPs). However, the conversion obtain from free enzyme retain at about 70% while the molar ratio increased from 10 to 25. Thus, the molar ratio of vinyl acetate to DMY was selected at 10 for both free ANL and ANL@PD-MNPs in the following experiment.

Temperature is a key parameter in the enzymatic acylation of DMY. With temperature increased from 30 to 45°C, the conversion rate increased from 40.3% to

67.1% (free ANL) and 69.6% to 79.1% (ANL@PD-MNPs) respectively (Fig.7C). Further increase in temperature had nearly no effect on the conversion rate. So the suitable temperature would be 45°C in the following experiment.

Also, enzyme concentration had a significant effect on the conversion yield. As shown in Fig.7D, when the amount of enzyme in the reaction mixture was increased from 10U to 40U, the conversion rate increased obviously for both free ANL (40.1% to 50.4%) and ANL@PD-MNPs (65.3% to 78.7%). However, further increase in ANL@PD-MNPs concentration had little effect on the conversion yield and the conversion rate retained 78%, indicating that the enzyme was saturated at 40 U in the reaction. In contrast, free ANL was statured at 80U and the corresponding conversion rate was 65% , which manifested the ANL@PD-MNPs have better catalytic capacity than free ANL.

Since the ANL@PD-MNPs could easily be isolated from the reaction system in an external magnetic field, its operational stability was investigated during ten cycles of re-use (Fig. 8). The ANL@PD-MNPs retained more than 90% of its original catalytic activity in the regioselective acylation of DMY after four consecutive reaction cycles and 56% of the initial activity after ten cycles of reuse. This result strongly suggests that the ANL@PD-MNPs is applicable to repeated use as a biocatalyst.

4. Conclusion

MNPs were successfully modified via a mussel-inspired polydopamine coating and characterized in terms of their morphology, composition, structure and magnetic

properties. The PD-MNPs proved to be suitable for ANL immobilization with high protein loading and good activity recovery. The prepared ANL@PD-MNPs manifested improved pH, thermal, solvent and storage stabilities compared with its free counterpart. Kinetic study of both immobilized and free enzymes showed that ANL@PD-MNPs had high catalytic efficiency. Significantly, the as-prepared ANL@PD-MNPs exhibited excellent reusability with over 55% of its initial activity after 10 cycles of consecutive reuse during the regioselective acylation process of DMY as well as the facility for convenient magnetic recovery of the biocatalyst.

Acknowledgements

We wish to thank the Program of State Key Laboratory of Pulp and Paper Engineering (2015C04), the National Natural Science Foundation of China (21336002; 21222606; 21376096), the Key Program of Guangdong Natural Science Foundation (S2013020013049), and the Fundamental Research Funds for the Chinese Universities (2015PT002; 2015ZP009) for partially funding this work.

References

[1] Salihu A, Alam M Z. *Process Biochem*, 2015, 1: 86
[2] Masomian M, Rahman R N Z R, Salleh A B, Basri M. *Process Biochem*, 2013, 1: 169
[3] Shu Z, Duan M, Yang J, Xu L, Yan Y. *Biotechnol Progr*, 2009, 2: 409
[4] Sheldon R A. *Adv Synth Catal*, 2007, 8-9: 1289
[5] Cao S, Xu H, Li X, Lou W, Zong M. *Acs Sustain Chem Eng*, 2015, 7: 1589
[6] Guan N, Xu J, Wang L, Sun D. *Colloids and Surfaces A: Physicochemical and Engineering Aspects*, 2009, 1: 221
[7] Yang Z, Zhang C, Zhang J, Bai W. *Biosens Bioelectron*, 2014, 2: 268
[8] Zhou J, Wang P, Wang C, Goh Y T, Fang Z, Messersmith P B, Duan H. *Acs Nano*, 2015, 7: 6951
[9] Haeshin L, Dellatore S M, Miller W M, Messersmith P B. *Science*, 2007, 5849: 426
[10] Ryu J, Ku S H, Lee H, Park C B. *Adv Funct Mater*, 2010, 13: 2132

[11] Zhou J, Wang C, Wang P, Messersmith P B, Duan H. *Chem Mater*, 2015, 8: 3071
[12] Liu Y, Ai K, Lu L. *Chem Rev*, 2014, 9: 5057
[13] Shi J, Yang C, Zhang S, Wang X, Jiang Z, Zhang W, Song X, Ai Q, Tian C. *Acs Appl Mater Inter*, 2013, 20: 9991
[14] Ni K, Lu H, Wang C, Black K C L, Wei D, Ren Y, Messersmith P B. *Biotechnol Bioeng*, 2012, 12: 2970
[15] Ren Y, Rivera J G, He L, Kulkarni H, Lee D K, Messersmith P B. *Bmc Biotechnol*, 2011,11: 63
[16] Yi S, A Kerstin L, Claudia G, Xuesi M S, Igor S, Richard W O, Jing L. *Journal of Neuroscience*, 2012, 1: 390
[17] Li W, Wu H, Liu B, Hou X, Wan D, Lou W, Zhao J. *J Biotechnol*, 2015, 4: 31
[] Bradford M M. *Anal Biochem*, 1976, 72: 248
[19] Gupta N, Rathi P, Gupta R. *Anal Biochem*, 2002, 1: 98
[20] Lundin A, Arner P, Hellmér J. *Anal Biochem*, 1989, 1: 125
[21] Kong J, Yu S. *Acta Bioch Bioph Sin*, 2007, 8: 549
[22] Zhang S, Zhang Y, Bi G, Liu J, Wang Z, Xu Q, Xu H, Li X. *J Hazard Mater*, 2014, 4: 27
[23] Li C Y, Wang W C, Xu F J, Zhang L Q, Yang W T. *J Membrane Sci*, 2011, 1: 7
[24] Si J, Yang H. *Mater Chem Phys*, 2011, 3: 519
[25] Wang Y, Wang S, Niu H, Ma Y, Zeng T, Cai Y, Meng Z. *J Chromatogr a*, 2013, 9: 20
[26] Qin H, Wang C M, Dong Q Q, Zhang L, Zhang X, Ma Z Y, Han Q R. *J Magn Magn Mater*, 2015, 6: 120
[27] Cao S, Li X, Lou W, Zong M. *J Mater Chem B*, 2014, 34: 5522
[28] Gagnon P, Toh P, Lee J. *J Chromatogr a*, 2014, 1: 171
[29] Ball V, Frari D D, Toniazzo V, Ruch D. *J Colloid Interf Sci*, 2012, 1: 366
[30] Xiao F, Feng C, Jin C, Liu X, Pan L, Xia A. *Mater Lett*, 2014, 6: 103
[31] Tahmasebi E, Yamini Y, Moradi M, Esrafili A. *Anal Chim Acta*, 2013, 1: 68
[32] Yakup Arica M, Soydogan H, Bayramoglu G. *Bioproc Biosyst Eng*, 2010, 2: 227
[33] Akg L S, Ka Ar Y, Denizli A, Ar Ca M Y. *Food Chem*, 2001, 3: 281
[34] Polizzi K M, Bommarius A S, Broering J M, Chaparro-Riggers J F. *Curr Opin Chem Biol*, 2007, 2: 220
[35] Kikani B A, Pandey S, Singh S P. *Bioproc Biosyst Eng*, 2013, 5: 567
[36] Kumar D, Nagar S, Bhushan I, Kumar L, Parshad R, Gupta V K. *Journal of Molecular Catalysis B: Enzymatic*, 2013, 6: 51
[37] Wang J, Zhao G, Jing L, Peng X, Li Y. *Biochem Eng J*, 2014, 9:226
[3] Feng J, Liu J, Ji L. *Biochimie*, 200, 9: 1337
[39] Gu H, Yu A, Chen H. *J Electroanal Chem*, 2001, 1: 119
[40] Telbisz Á, Müller M, özvegy-Laczka C, Homolya L, Szente L, Váradi A, Sarkadi B. *Biomembranes*, 2007, 11: 269
[41] Goormaghtigh E, Cabiaux V, Ruysschaert J M. *Eur J Biochem*, 1990, 2: 409
[42] Surewicz W K, Mantsch H H, Chapman D. *Biochemistry-Us*, 1993, 2: 39
[43] Mechelke M, Habeck M. *Proteins: Structure, Function, and Bioinformatics*, 2013, 6: 94
[44] Dong A, Jones L S, Kerwin B A, Krishnan S, Carpenter J F. *Anal Biochem*, 2006, 2: 22

Figure Captions

Figure 1 TEM images and size distribution of MNPs (A), PD-MNPs (B) and ANL@PD-MNPs (C). The polymerization time for the PD-MNPs was 1 h.

Figure 2 FTIR spectra for MNPs (a) and PD-MNPs (b).

Figure 3 XRD patterns of the MNPs and PD-MNPs (2.5 mg/mL dopamine hydrochloride).

Figure 4 Effects of immobilization conditions on the activity recovery and the protein loading. (A) Effect of pH (1.5 mg lipase, .3 mg PD-MNPs, 2.5mg/mL dopamine hydrochloride, polymerization time 1h; immobilization time 9 h)； (B) Effect of immobilization time (1.5 mg lipase, .3 mg PD-MNPs, 2.5mg/mL dopamine hydrochloride, polymerization time 1h; pH .0).

Figure 5 Optimal pH and temperature of ANL@PD-MNPs and free lipase.

Figure 6 Stabilities of ANL@PD-MNPs and free lipase. (A) pH stability; (B)Thermal stability; (C) Storage stability; (D) Solvent tolerance

Figure 7 (A)The time course in enzymatic regioselective acylation of DMY catalyzed by ANL@PD-MNPs and free lipase (2 mL DMSO, 0.04 mM DMY, 0.4 mM vinyl acetate, 35 °C, 200 rpm, 60U ANL@PD-MNPs or free ANL); (B) The effect of the molar ratio of substrates on the conversion yield (2 mL DMSO, 35 °C, 200 rpm, 60U ANL@PD-MNPs or free ANL); (C) The effect of the temperature on the conversion yield (2 mL DMSO, 0.04 mM DMY, 0.4 mM vinyl acetate , 200 rpm, 60U ANL@PD-MNPs or free ANL); (D) The effect of the enzyme concentration on the conversion yield (2 mL DMSO, 0.04 mM DMY, 0.4 mM vinyl acetate , 200 rpm, 45°C);

Figure 8 The operational stability of ANL@PD-MNPs.

Table 1 Results of amide I band deconvolution for free lipase and ANL@PD-MNPs

Sample	Secondary structure (%)			
	β-sheet	*α*-helix	random coli	*β*-turn
Free lipase	26.15	26.14	29.7	17.93
ANL@PD-MNPs	26.99	2.	27.46	16.67

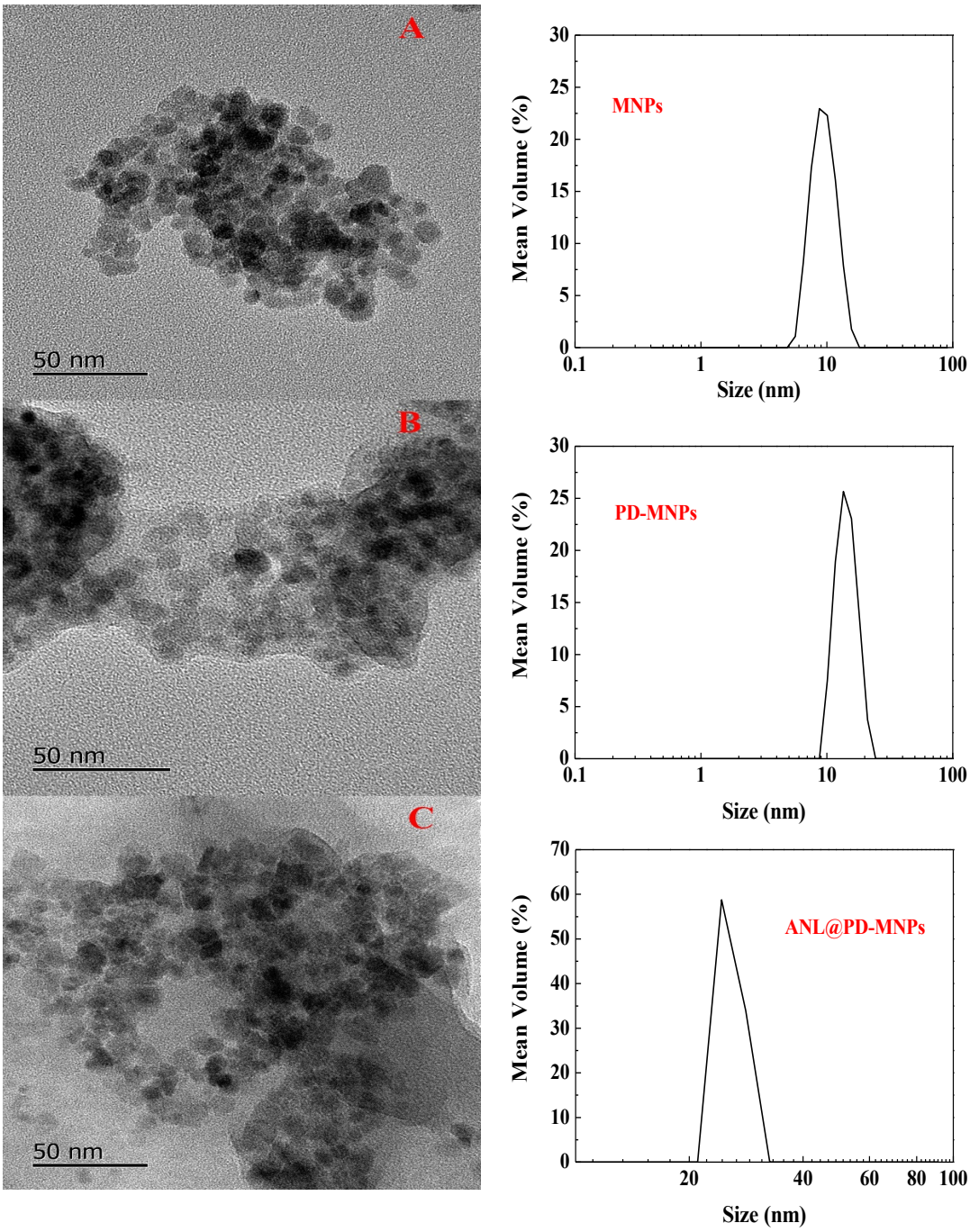

Deng X et al., Fig.1

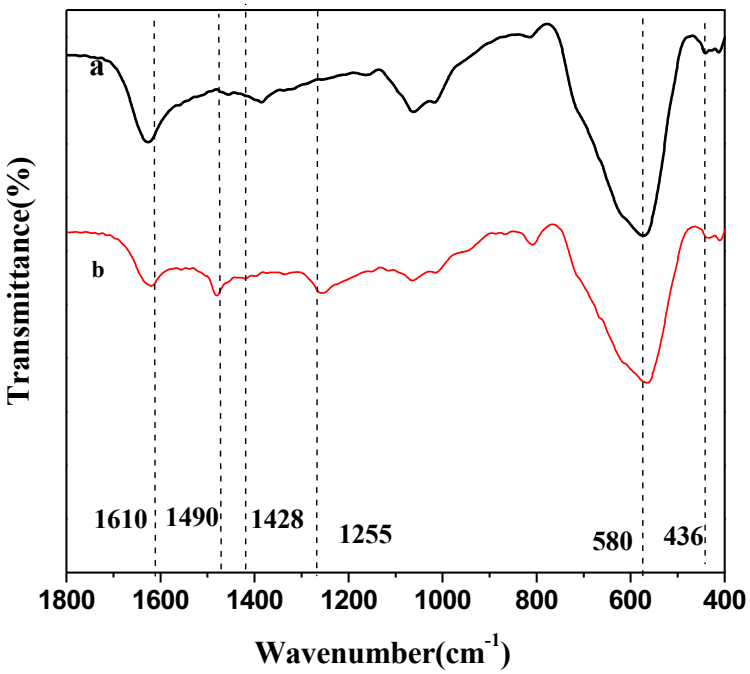

Deng X et al., Fig.2

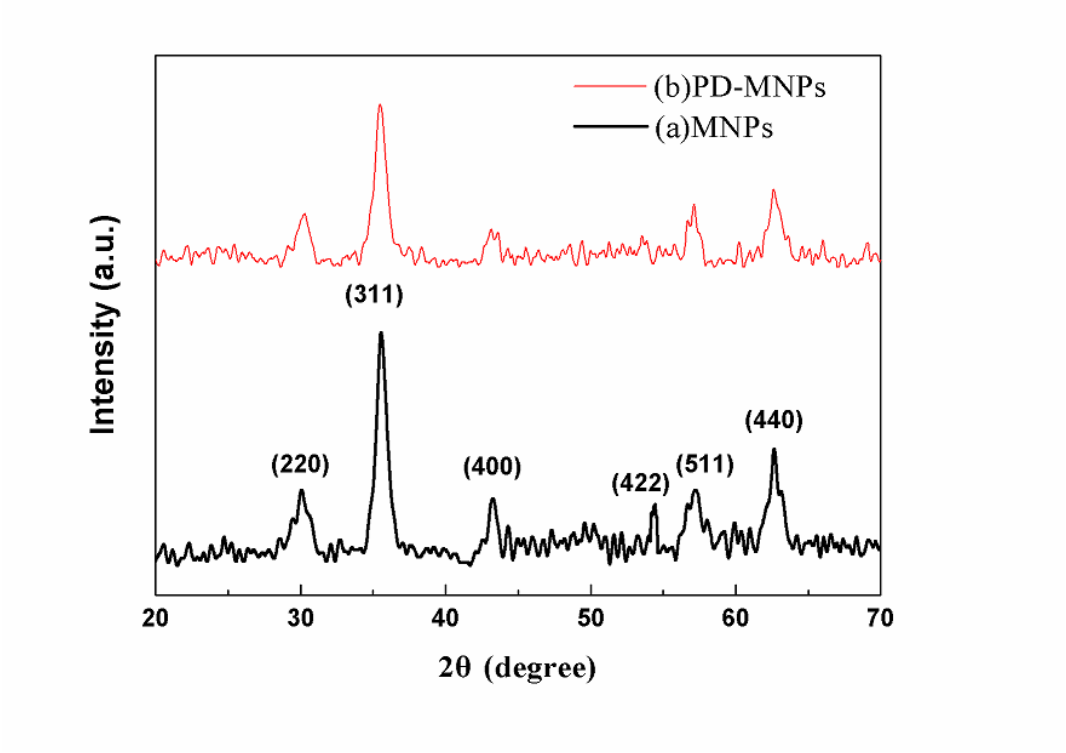

Deng X et al., Fig.3.

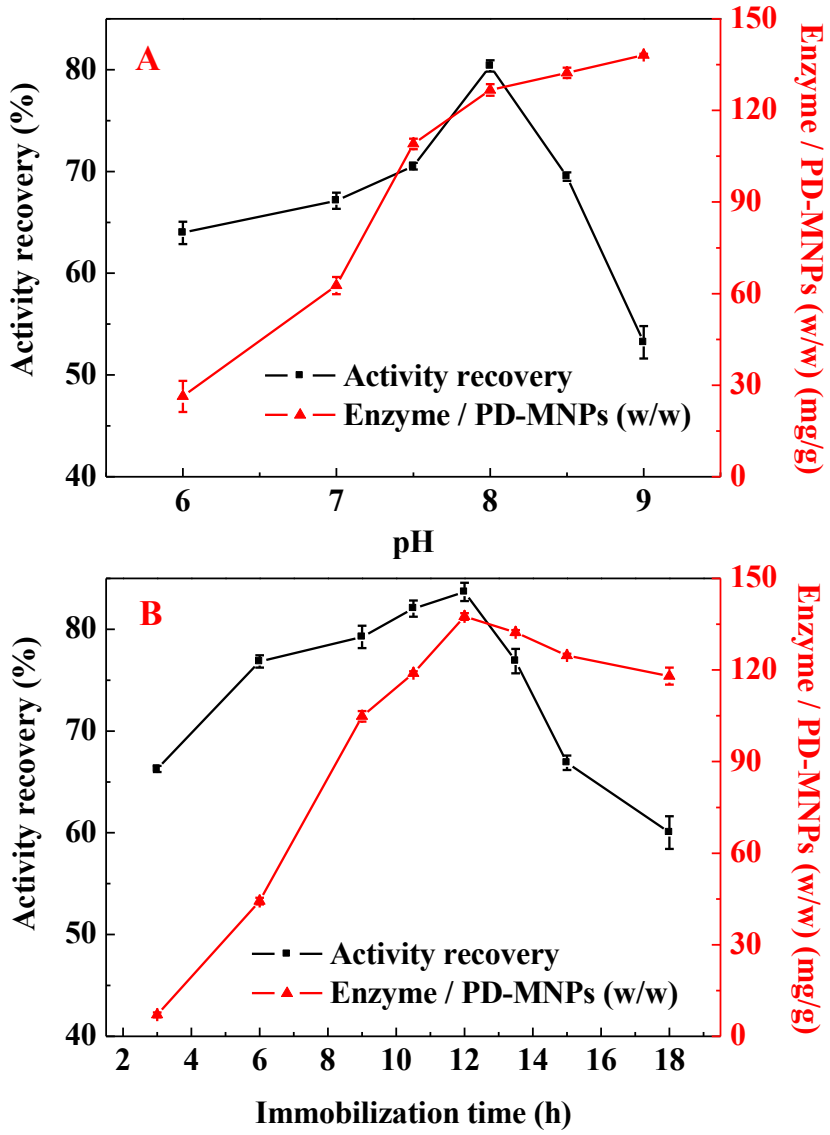

Deng X et al., Fig.4

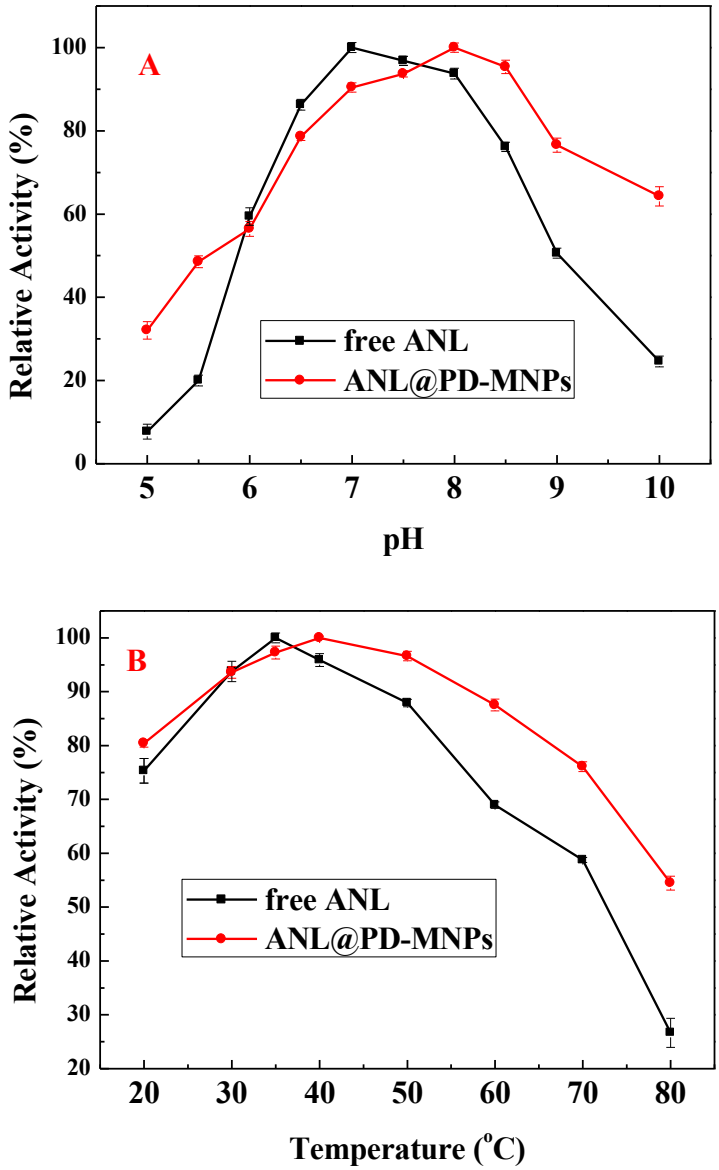

Deng X et al., Fig.5

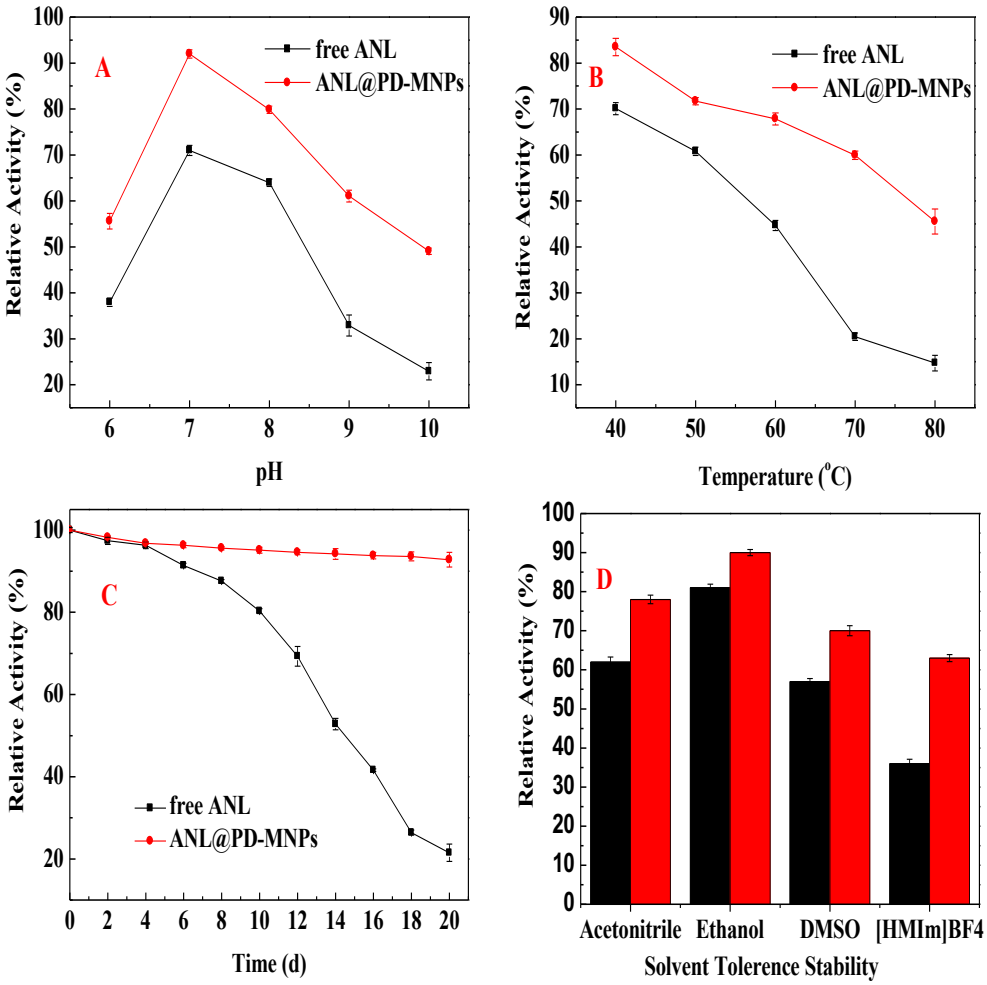

Deng X et al., Fig.6

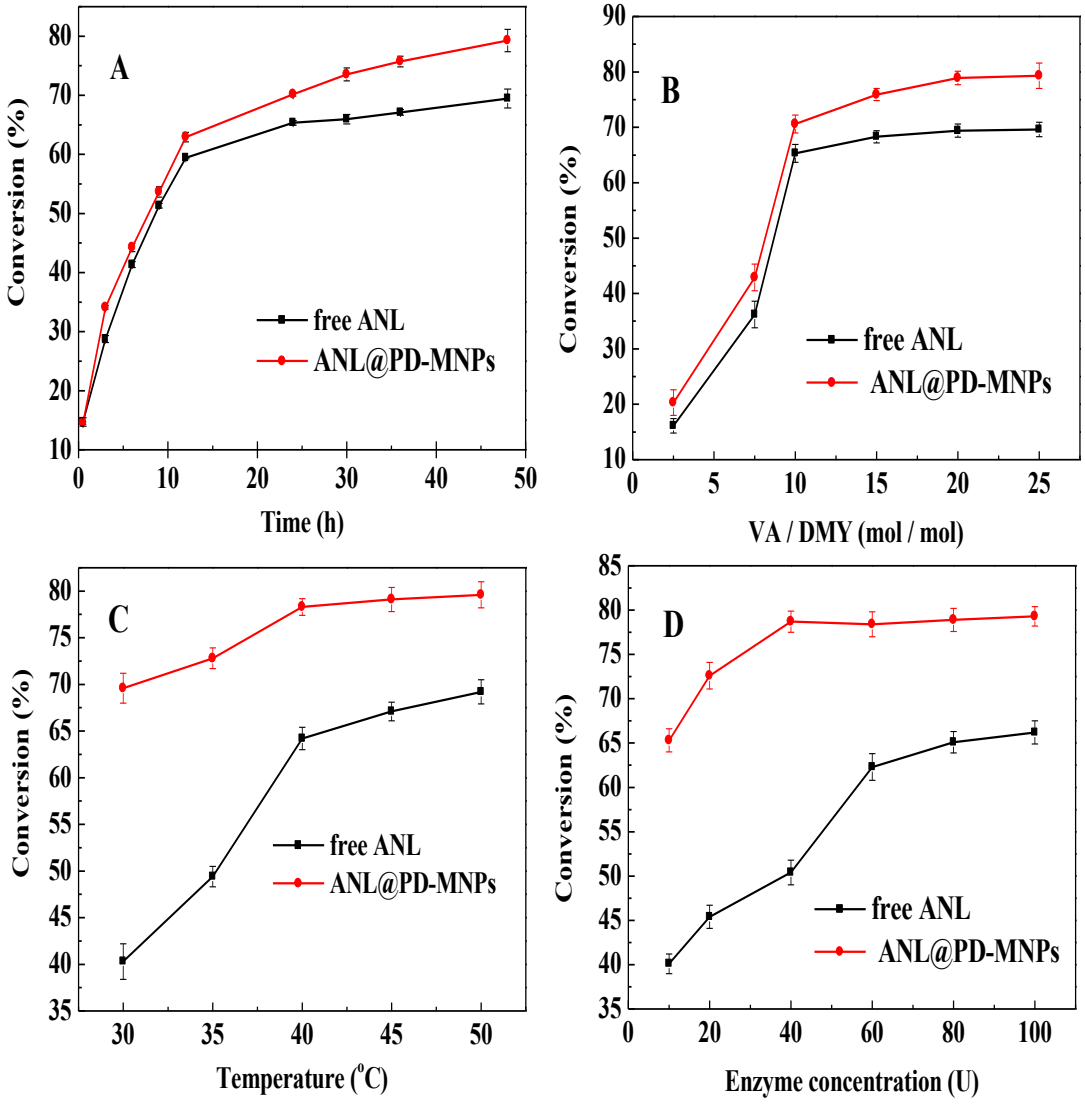

Deng X et al., Fig. 7

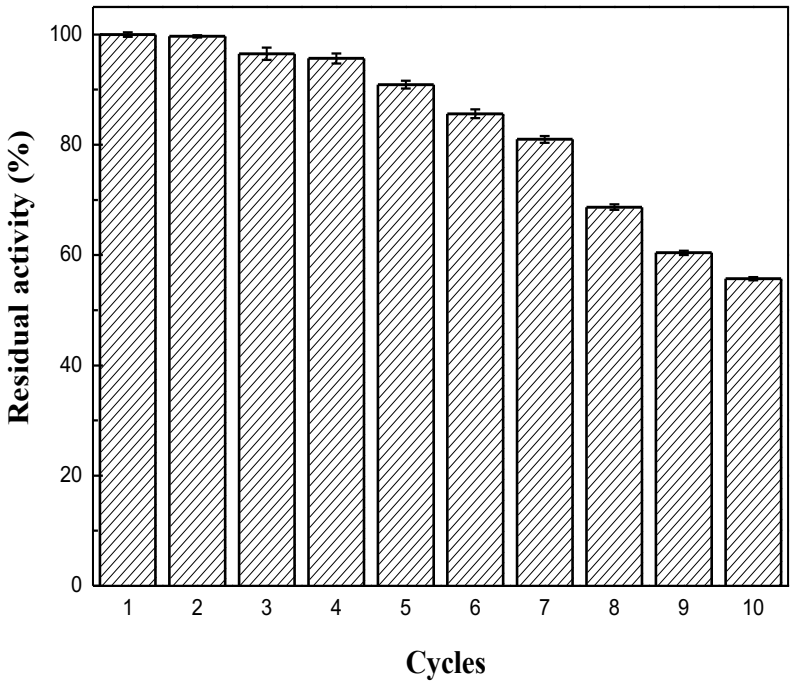

Deng X et al., Fig.

1 **Graphical abstract**

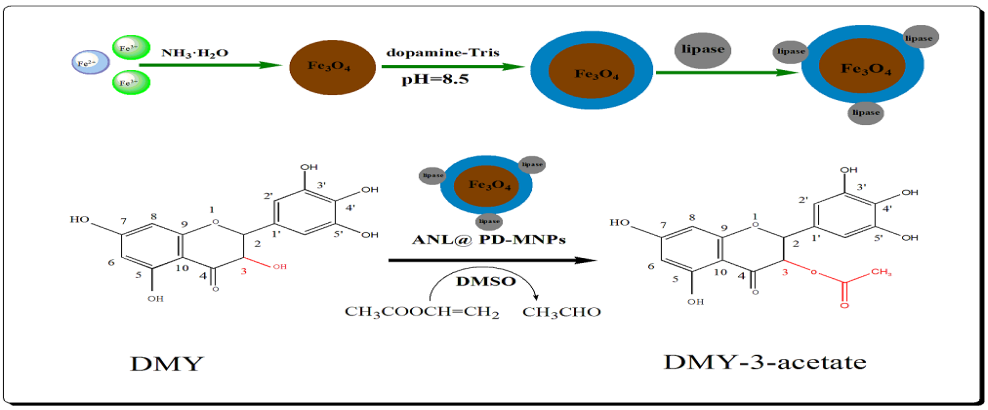

2

3

4